

Award Number: W81XWH-11-1-0248

TITLE: Echo-Planar Imaging-Based, J-Resolved Spectroscopic Imaging for Improved Metabolite Detection in Prostate Cancer

PRINCIPAL INVESTIGATOR: Michael Albert Thomas Ph.D.

CONTRACTING ORGANIZATION: University of California, Los Angeles
Los Angeles, CA 90024-1406

REPORT DATE: October 2014

TYPE OF REPORT: Annual

PREPARED FOR: U.S. Army Medical Research and Materiel Command
Fort Detrick, Maryland 21702-5012

DISTRIBUTION STATEMENT: Approved for Public Release;
Distribution Unlimited

The views, opinions and/or findings contained in this report are those of the author(s) and should not be construed as an official Department of the Army position, policy or decision unless so designated by other documentation.

REPORT DOCUMENTATION PAGE			<i>Form Approved</i> <i>OMB No. 0704-0188</i>		
Public reporting burden for this collection of information is estimated to average 1 hour per response, including the time for reviewing instructions, searching existing data sources, gathering and maintaining the data needed, and completing and reviewing this collection of information. Send comments regarding this burden estimate or any other aspect of this collection of information, including suggestions for reducing this burden to Department of Defense, Washington Headquarters Services, Directorate for Information Operations and Reports (0704-0188), 1215 Jefferson Davis Highway, Suite 1204, Arlington, VA 22202-4302. Respondents should be aware that notwithstanding any other provision of law, no person shall be subject to any penalty for failing to comply with a collection of information if it does not display a currently valid OMB control number. PLEASE DO NOT RETURN YOUR FORM TO THE ABOVE ADDRESS.					
1. REPORT DATE October 2014		2. REPORT TYPE Annual		3. DATES COVERED 30 Sep 2013 – 29 Sep 2014	
4. TITLE AND SUBTITLE 9W cID`UbUf`a Uj]b[!6 UgyXZ>!FYgc`j YX`GdYWFcgWtd]W-a Uj]b[`Zf`-a dfcj YX` Metabolite Detection in Prostate Cancer "			5a. CONTRACT NUMBER		
			5b. GRANT NUMBER W81XWH-11-1-0248		
			5c. PROGRAM ELEMENT NUMBER		
6. AUTHOR(S) Michael Albert Thomas Ph.D. E-Mail: athomas@mednet.ucla.edu			5d. PROJECT NUMBER		
			5e. TASK NUMBER		
			5f. WORK UNIT NUMBER		
7. PERFORMING ORGANIZATION NAME(S) AND ADDRESS(ES) AND ADDRESS(ES) University of California, Los Angeles Los Angeles, CA 90024-1406			8. PERFORMING ORGANIZATION REPORT NUMBER		
The OCGA 11000 Kinross Ave. Suite#211 Los Angeles, CA 90095					
9. SPONSORING / MONITORING AGENCY NAME(S) AND ADDRESS(ES) U.S. Army Medical Research and Materiel Command Fort Detrick, Maryland 21702-5012			10. SPONSOR/MONITOR'S ACRONYM(S)		
			11. SPONSOR/MONITOR'S REPORT NUMBER(S)		
12. DISTRIBUTION / AVAILABILITY STATEMENT Approved for Public Release; Distribution Unlimited					
13. SUPPLEMENTARY NOTES					
14. ABSTRACT Purpose: 1) To implement an echo-planar imaging (EPI)-based 2D J-resolved spectroscopy on a 3T MRI/MRS scanner;2) To evaluate the multi-voxel 2D J-resolved echo-planar spectroscopic imaging (EP-JRESI) in malignant PCa patients, benign prostatic hyperplasia (BPH) patients and healthy prostates. 3) To develop and further optimize the ProFit algorithm to post-process the multi-dimensional MRS data from different prostate pathologies. Scope: Improved cancer detection (specificity) in differentiating malignant from benign prostate cancer will be achieved using a novel four-dimensional (4D) EP-JRESI. Improved spectroscopic imaging techniques will enable unambiguous detection of metabolites and the lipids in situ, which could potentially complement the existing diagnostic modalities commonly used in prostate cancer. Progress and Major Findings: After successful implementation of the 4D EP-JRESI sequence on a 3T MRI scanner, the 4D EP-JRESI data were recorded in several patients and healthy males during the first two years. Eleven more male subjects (6 patients and 5 healthy) were investigated using endorectal as well as external MRI coils and the findings are reproducible with that obtained in the past years. A manuscript was peer-reviewed by a leading MR journal during the last year.					
15. SUBJECT TERMS: Digital Rectal Examination, prostate specific antigen, Four Dimensional (4D) Echo-Planar J-Resolved Spectroscopic Imaging (EP-JRESI); Citrate, Choline, Creatine, Spermine, 3Tesla MRI scanner, Endo-rectal MR coil, WET Water Suppression, prostate cancer (PCa), benign prostatic hyperplasia (BPH), prior-knowledge fitting					
16. SECURITY CLASSIFICATION OF:			17. LIMITATION OF ABSTRACT	18. NUMBER OF PAGES	19a. NAME OF RESPONSIBLE PERSON USAMRMC
a. REPORT U	b. ABSTRACT U	c. THIS PAGE U			19b. TELEPHONE NUMBER (include area code)
			UU	37	

Table of Contents

	Page
Introduction.....	4
Body.....	4
Key Research Accomplishments.....	6
Reportable Outcomes.....	6
Conclusion.....	7
References.....	7
Appendices.....	9

Introduction: Prostate cancer (PCa) is the most common cancer in men in several countries, with the American Cancer Society (ACS) estimating 241,740 new cases of PCa to be diagnosed and deaths of 28,170 men of PCa (1). Due to its prevalence in the male population as well as its unpredictable clinical course, early detection and diagnosis have become a priority for many health care professionals. Another method for staging prostate cancer is through imaging techniques including ultrasound, computed tomography (CT), and magnetic resonance imaging (MRI) with or without the help of dynamic contrast enhancement modeling (DCE-MRI), diffusion weighted imaging (DWI), and magnetic resonance spectroscopy (MRS) (2-5). MRS is a powerful tool for exploring the cellular chemistry of human tissues (3,5,6-11). There is a growing body of evidence that ¹H MRS may contribute to the clinical evaluation of prostate cancer and also for evaluating the metabolic alterations due to therapy. There have been no reports on combining two spectral dimensions with two-dimensional (2D) or three dimensional (3D) spatial encoding applicable to prostate cancer. Acceleration of magnetic resonance spectroscopic imaging (MRSI) has been demonstrated using echo-planar imaging techniques (12-13). Recently, Schulte et al. have successfully developed an algorithm called prior-knowledge fitting (ProFit) to quantify metabolite concentrations using the JPRESS spectra recorded using a Philips 3T MRI scanner (14). It was demonstrated that metabolite quantitation of JPRESS spectra with ProFit was accurate, robust and yielding generally consistent results, both *in vivo* and *in vitro*. Their results suggest that the number of quantifiable prostate metabolites can be increased from 3-4 with 1D PRESS/LC-Model to more than 10 with JPRESS/ProFit (15-16).

Body:

i) Proposed Task 1 (Months 1-6): *To implement a multi-voxel based extension of the JPRESS sequence, in which two spectral encodings will be combined with two spatial encodings using the new Siemens VB17a platform. This four-dimensional (4D) data acquisition scheme will be accomplished utilizing the EPI approach that is commonly used for spatial encoding in MRI.*

Completed and Reported in the 1st year Annual Report.

ii) Proposed Task 2: *To evaluate the EPI-based JPRESS using a prostate phantom containing several metabolites which have been reported in prostate tissues, and to optimize the EP-JJRESI sequence and other acquisition parameters using the phantom (Months 6-12).*

Completed and Reported in the 1st year Annual Report.

iv) Proposed Task 3: *To record the 4D EP-JRESI spectra in the peripheral, central and transition zones of healthy prostates. (Months 6-18).*

Five more healthy males have been investigated.

Proposed Task 4: *To develop, evaluate and optimize the prior-knowledge basis set spectra using the GAMMA-simulation and prostate phantom solutions as prior knowledge for the multi-voxel based JPRESS spectra recorded using the 3T MRI scanner (Months 6-12).*

Accomplished during September 29, 2011-October 28 2012:

Proposed Task 5: To record the multi-voxel-based 2D spectra in the peripheral, central and transition zones of patients with BPH and malignant prostate cancer. The prostate metabolite concentrations calculated using the ProFit algorithm prepared for the multi-voxel data will be compared with LC-Model processed 1D spectral based MRSI data (**Months 18-36**).

Accomplished during October 29, 2013-October 28 2014: Six malignant prostate cancer patients and five healthy males were investigated during the current year. The 4D EP-JRESI data were recorded using the following parameters: TR/TE=1.5s/30ms, 2 averages, 512 t_2 , oversampled $32k_x$, 64 increments along the indirect spectral (t_1) and 16 spatial k_y dimensions; the endorectal "receive" coil. The oversampled $32k_x$ were processed to normal $16k_x$ points. First, the 4D NUS EP-JRESI data was acquired in a 71 year old PCa patient; Extracted 1ml spectra from 3 different locations after the CS reconstruction are shown in Figure 1 (ii, iii and iv) and the middle insert (i) shows the multi-voxel grids overlaid on an T_2W axial MRI slice.

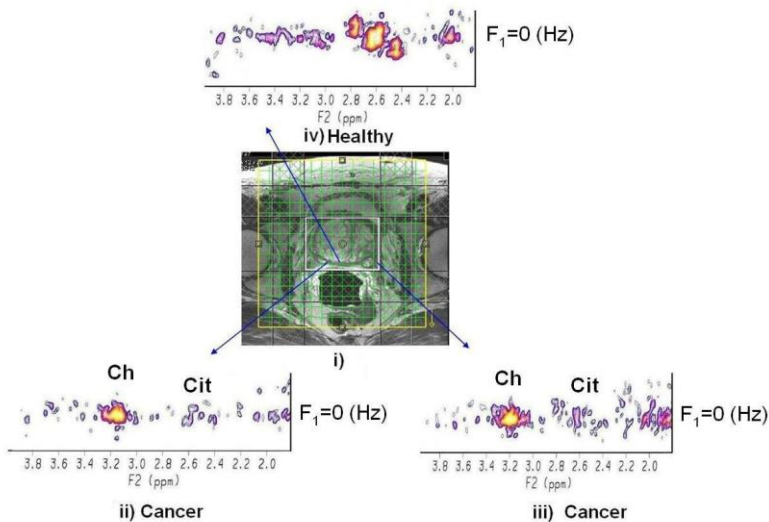
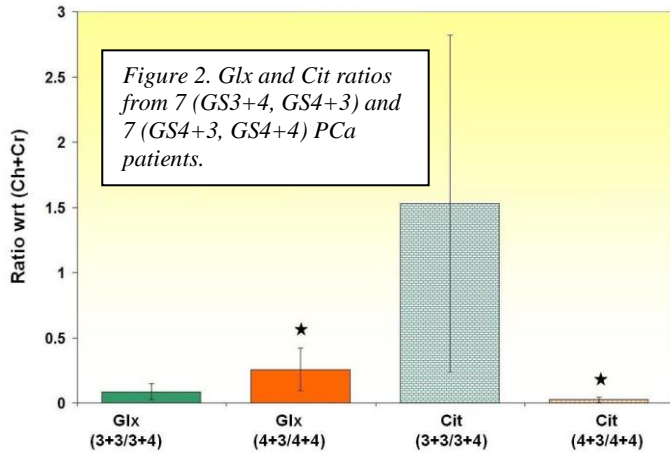


Figure 1. i) Axial T_2W slice showing the multi-voxel EP-JRESI grids; extracted 2D JPRESS spectra of malignant voxels (ii) and (iii), and the healthy voxel in the peripheral zone (iv).



We were able to reproduce the above mentioned findings in more patients with known GS, and also, in remaining four patients whose histology findings were not known. 2D peak (cross and diagonal) volumes were defined by the operator in the frequency domain 2D JPRESS data for this pilot analysis. Two different ratios were calculated using the 4D NUS EP-JRESI data acquired in 14 PCa patients: (Glx/(Ch+Cr+Spm) and

Cit/(Ch+Cr+Spm), one set from the affected lesions and another set from the contralateral healthy sides. As evident in Fig.2, additional metabolite (Glx) changes can be detected using the 4D NUS EP-JRESI data. Both ratios showed significant changes ($p < 0.05$); however, this outcome from a small group of PCa patients needs to be treated with caution showing a necessity for further research using larger patient cohorts.

Key Research Accomplishments

- Continued evaluation of the 4D EP-JRESI sequence in 6 malignant prostate cancer patients and five healthy male subjects.
- We have made further progress on compressed sensing reconstruction of the non-uniformly undersampled 4D EP-JRESI sequence using different reconstruction methods such as maximum entropy, total variation (TV), etc . This will facilitate shortening the endorectal spectral acquisition and reducing the patient inconvenience during the scan. A manuscript was submitted to NMR in Biomedicine and a major revision is in progress.
- Using the preliminary results obtained using this IDEA grant, we had reported our NIH R01 grant application submission entitled “Fast J-resolved Prostate MR Spectroscopic Imaging and Non-linear Reconstruction” was resubmitted on July 5, 2014 using the preliminary results from this IDEA grant. The percentile score was 37% and we plan to resubmit this grant to NIH.

Reportable Outcomes:

A. Peer-reviewed Publications:

1. Nagarajan R, Iqbal Z, Burns B, et al. Accelerated Echo Planar J-Resolved Spectroscopic Imaging in Prostate Cancer: Nonlinear Reconstruction Using Total Variation And Maximum Entropy. NMR in Biomedicine 2014 [being revised].

B. Presentations: During the 3rd year, three abstracts were presented at the 23rd International Society of Magnetic Resonance in Medicine (ISMRM), Milan, Italy, May 10-16, 2014: the first abstract entitled “Accelerated Echo Planar J-Resolved Spectroscopic Imaging in Prostate Cancer: Nonlinear Reconstruction Using Total

Variation And Maximum Entropy” (oral presentation), #962; the 2nd abstract entitled “Maximum Entropy Reconstructed Echo Planar J-Resolved Spectroscopic Imaging and Diffusion Weighted Imaging in Prostate Cancer” (eposter), # 4108; the 3rd abstract entitled “Compressed Sensing based Echo-planar 3D MRSI Using Short Echo Time: A Pilot Evaluation Using a Prostate Phantom” (poster), # 1529 summarizing the implementation of a novel 3D EPSI sequence and evaluation of it using a prostate phantom.

C. Books: None on Prostate Cancer Research based.

Conclusions: After successfully implementing the 4D EP-JRESI scanning protocol on the 3T MRI scanner and testing it in healthy controls and patients during the earlier 2 years, 11 more subjects have been investigated in the 3rd year. We will continue to recruit 10 malignant and 5 benign prostate cancer patients, and 5 healthy male subjects during the next year (no-cost time extension).

References

- 1) Dall’era MA, Cooperberg MR, Chan JM, *et al.* Active surveillance for early-stage prostate cancer: review. *Cancer*. 2008 Apr 15;112(8):1650-9. **PMID: 18306379**
- 2) McNeal JE. Normal histology of the prostate. *Am J Surg Pathol* 1988;12:619-633. **PMID: 2456702**
- 3) Weinreb JC, Blume JD, Coakley FV, *et al.* Prostate cancer: sextant localization at MR imaging and MR spectroscopic imaging before prostatectomy--results of ACRIN prospective multi-institutional clinicopathologic study. *Radiology*. 2009 Apr;251(1):122-33. **PMID: 19332850**
- 4) Jacobs MA, Ouwerkerk R, Petrowski K and Macura KJ. Diffusion-weighted imaging with apparent diffusion coefficient mapping and spectroscopy in prostate cancer. *Top Magn Reson Imaging*. 2008;19:261-72 **PMID:19512848**
- 5) Scheenen TW, Heijmink SW, Roell SA, *et al.* Three-dimensional proton MR Spectroscopy of human prostate at 3T without endorectal coil: feasibility. *Radiology* 2007;245:507-16. **PMID: 17848681**
- 6) Thomas MA, Narayan P, Kurhanewicz J, Jajodia P, Weiner MW. 1H MR spectroscopy of normal and malignant human prostates in vivo. *J Magn Reson* 1990; 87:610–619. **PMID:N/A**
- 7) Thomas MA, Narayan P, Kurhanewicz J, *et al.* Detection of phosphorus metabolites in human prostates with a transrectal ³¹P NMR probe. *J Magn Reson* 1992; 99: 377-386. **PMID: N/A**
- 8) Narayan P, Kurhanewicz J. Magnetic Resonance spectroscopy in prostate disease: diagnostic possibilities and future developments. *Prostate* 1992; Suppl 4: 43-50. **PMID: 1374177**
- 9) van der Graaf M, Schipper RG, Oosterhof GO, J.A. Schalken, AA. Proton MR spectroscopy of prostatic tissue focused on the detection of spermine, a possible biomarker of malignant behavior in prostate cancer. *MAGMA* 2000; 10(3):153-9. **PMID: 10873205**
- 10) Jordan KW and Cheng LL. NMR-based metabolomics approach to target biomarkers for human prostate cancer. *Expert Rev Proteomics* 2007;4:389-400. **PMID: 17552923**

- 11) Kurhanewicz J, Swanson MG, Nelson SJ, and Vigneron DB. Combined magnetic resonance imaging and spectroscopic imaging approach to molecular imaging of prostate cancer. *J Magn Reson Imaging* 2002;16(4):451-463. **PMID: 12353259**
- 12) Mansfield P. Spatial mapping of the chemical shift in NMR. *Magn Reson Med* 1984; 1: 370 – 386. PMID:6571566
- 13) Posse S, Otazo R, Caprihan A, et al. Proton echo-planar spectroscopic imaging of J-coupled resonances in human brain at 3 and 4 Tesla. *Magn Reson Med* 2007; 58(2): 236-44. PMID: 17610279
- 14) Schulte RF and Boesiger P. ProFit: two-dimensional prior-knowledge fitting of J-resolved spectra. *NMR Biomed* 2006;19:255-263. **PMID: 16541464**
- 15) Lange T, Schulte RF and Boesiger P. Quantitative J-resolved prostate spectroscopy using two-dimensional prior-knowledge fitting. *Magn Reson Med* 2008;59:966-972. PMID: 18429013
- 16) Thomas MA, Lange T, Velan SS, et al. Two-dimensional MR Spectroscopy of healthy and cancerous prostates in vivo. *Magn Reson Mater Phy (MAGMA)* 2008;21(6):443-58. **PMID: 18633659**
- 17) Wright A, Tessem MB, Bertilsson H, et al. Quantitative ¹H HR-MAS using LC Model shows glutamate, choline, glycerylphosphocholine, and glucose as biomarkers of prostate. *Proc Intl Soc Magn Reson Med* 2012;20:2975. **PMID: N/A**
- 18) Stenman K, Hauksson JB, Grobner G, et al. Detection of polyunsaturated omega-6 fatty acid in human malignant prostate tissue by 1D and 2D high resolution magic angle spinning NMR spectroscopy. *MAGMA* 2009;22:327-31 **PMID: 19921294.**

Appendix:

1. Nagarajan R, Iqbal Z, Burns BL, et al. Accelerated Echo Planar J-Resolved Spectroscopic Imaging In Prostate Cancer: Nonlinear Reconstruction Using Total Variation And Maximum Entropy. 22nd ISMRM, Milan, Italy, May 10-16, 2014, #962.
2. Nagarajan R, Iqbal Z, Burns BL, et al. Maximum Entropy Reconstructed Echo Planar Based Spectroscopic Imaging and Diffusion Weighted Imaging In Prostate Cancer. 22nd ISMRM, Milan, Italy, May 10-16, 2014, #4108.
3. Nagarajan R, Wilson N, Thomas MA. Compressed Sensing Based Echo Planar 3D MRSI Using Short Echo Time: A Pilot Evaluation Using A Prostate Phantom. 22nd ISMRM, Milan, Italy, May 10-16, 2014, #1529.
4. Nagarajan R, Iqbal Z, Burns B, et al. Accelerated Echo Planar J-Resolved Spectroscopic Imaging in Prostate Cancer: Nonlinear Reconstruction Using Total Variation And Maximum Entropy. *NMR in Biomed* 2014 (revised after the 1st review).

ACCELERATED ECHO PLANAR J-RESOLVED SPECTROSCOPIC IMAGING IN PROSTATE CANCER: NONLINEAR RECONSTRUCTION USING TOTAL VARIATION AND MAXIMUM ENTROPY

Rajakumar Nagarajan¹, Zohaib Iqbal¹, Brian Burns¹, Neil Wilson¹, Manoj K Sarma¹, Daniel A Margolis¹, Robert E Reiter², Steven S Raman¹, and M.Albert Thomas¹
¹Radiological Sciences, University of California Los Angeles, LOS ANGELES, CA, United States, ²Urology, University of California Los Angeles, LOS ANGELES, CA, United States

Target audience: MR pulse sequence developers, scientists/clinicians interested in accelerated imaging and non-linear reconstruction in prostate imaging

Introduction: Prostate cancer is the second leading cause of cancer death in men next to lung cancer. The American Cancer Society's estimates 238,590 new cases and 29,720 deaths from prostate cancer in 2013 (1). One in 6 men will get prostate cancer during his lifetime and one in 36 will die of this disease. Current limitations of single voxel and multivoxel prostate spectroscopic imaging are due to the overlap of metabolite resonances, quantifying few metabolites only (citrate (Cit), choline (Ch), creatine (Cr) and spermine (Spm)) and long echo times. A single-voxel based two-dimensional (2D) J resolved spectroscopic sequence (JPRESS) has been implemented and demonstrated in prostate cancer, and showed improved spectral dispersion due to the added spectral dimension (2,3). Compressed sensing was recently introduced as a powerful method to accelerate MRI by exploiting the sparsity of the images in a known transform domain to reconstruct non-uniformly undersampled (NUS) k-space data (4). By combining EPSI with JPRESS, 2D spectra can be recorded in multiple locations in prostate using four dimensional (4D) Echo-Planar J-Resolved Spectroscopic Imaging (EP-JRESI) combining 2 spectral with 2 spatial dimensions. A pilot feasibility was demonstrated recently to map metabolites in the human prostate (5). Maximum entropy (MaxEnt) and total variation (TV) image reconstruction have been used to reconstruct NUS indirect spectral and spatial dimensions (6). The goal of the present work was to compare and correlate the significant metabolites of the accelerated 4D EP-JRESI data acquired in prostate cancer and reconstructed with MaxEnt and TV.

Materials and Methods: Twenty two prostate cancer patients with a mean age of 63.8 years (range: 46–79 years) were investigated in this study. Prostate-specific antigen (PSA) varied from 0.7 to 22.8 ng/mL (mean of 6.23 ng/mL) and the mean delay between biopsy and MR investigation was 8 weeks. This study was approved by the Institutional Review Board, and informed consent was obtained from each patient. A Siemens 3T MRI Scanner with high-performance gradients (Trio-Tim, Siemens Medical Solutions, Erlangen, Germany) was used in this investigation. A 4D NUS EP-JRESI sequence was implemented on the 3T MRI scanner and the volume of interest (VOI) was localized using three slice-selective radio-frequency (RF) pulses (90°-180°-180°). The total time for obtaining a fully sampled 4D EP-JRESI data (TR of 1.5s, 16ky*16kx, 64-100t₁, 512t₂) can be more than 25 minutes. The MaxEnt and TV reconstructions enable a stable and accurate reconstruction from the NUS based EP-JRESI data (25% of t₁ and k_y increments) with a reduced total time. The parameters for the EP-JRESI were: TR/TE/Av_g = 1.5s/30ms/1-2, 16 phase encoding steps, 512 complex points with an F₂ bandwidth of 1190Hz. For the second dimension (F₁), 64 increments with bandwidths of 1000Hz were used. A 4X NUS was imposed along the plane containing incremented spectral and spatial dimensions (t₁ and k_y). The individual voxel volume in human prostate was 1ml. Two sets of data were collected, one with water suppression (WS) with a total scan time of 6-12 minutes and second with non-water suppression (NWS) using 1 average only. The NUS data was reconstructed by MaxEnt and TV separately. A modified Split-Bregman algorithm (6) solves the unconstrained TV optimization problem as shown in Eqn.(1) below:

$$\min_m \|\nabla m\|_1 + \lambda \|F_u m - y\|_2 \quad (1)$$

where ∇ is the gradient operator, m is the reconstructed data, $\|x\|_1$ is the L₁-norm, λ is a regularization parameter, F_u is the under sampled Fourier transform, and y is the under-sampled data. The above equation removes the incoherent artifacts due to NUS by minimizing the total variation (TV) while maintaining consistency with the sampled measurements. MaxEnt is a constrained convex optimization algorithm that uses a variant of the conjugate gradient method to iteratively solve the inverse problem (6-8):

$$\text{maximize } S_{1/2}(f) \text{ s.t. } \|F^{-1} Kf - D\|_2 \leq \sigma \quad (2)$$

where f is the estimated fully-sampled spectrum at each iteration, F^{-1} is the inverse Fourier transform, K is the NUS matrix, D is the measured time-domain data, σ is the noise standard deviation, and $S_{1/2}(f)$ is the spin-1/2 entropy of the estimated spectrum (6-8).

Results and Discussion: All NUS based 4D EP-JRESI data were processed using TV and MaxEnt reconstruction with custom processing software. We observed decreased levels of Cit, Spm and mI with respect (Ch+Cr) in cancer locations compared to non-cancer locations in both TV and MaxEnt reconstruction. Also we have compared and correlated the TV with MaxEnt reconstruction methods of a few metabolites which showed significant decrease as well as decreasing trend in the cancer locations compared to non-cancer locations. Figure 1 shows the correlation of maxEnt and TV of Cit/(Ch+Cr) and Spm/(Ch+Cr) in cancer and non-cancer location. Similarly a positive correlation was found in the following metabolites in cancer locations: Cit/(Ch+Cr) (R²=0.8708), mI/(Ch+Cr) (R²=0.972) and Spm/(Ch+Cr) (R²=0.7348). Also we observed positive correlation of Spm and mI in non-cancer location. Table.1 shows the metabolites ratio of maxEnt and TV in cancer and non-cancer locations. There was an overlap between cancer and non-cancer locations, possibly due to the low signal-to-noise ratio of the Cr peak. In addition, Ch and Cr were not always well resolved especially in cancer locations, adding to the uncertainty. The advantage of NUS based 4D EP-JRESI sequence will record short TE-based spectra from multiple regions of a prostate and will show more metabolites, such as glutamate (Glu), glutamine (Gln), myo-inositol (mI), taurine (Tau), lactate (Lac), and choline groups, in addition to the normally detected Cit, Cr, Ch and Spm.

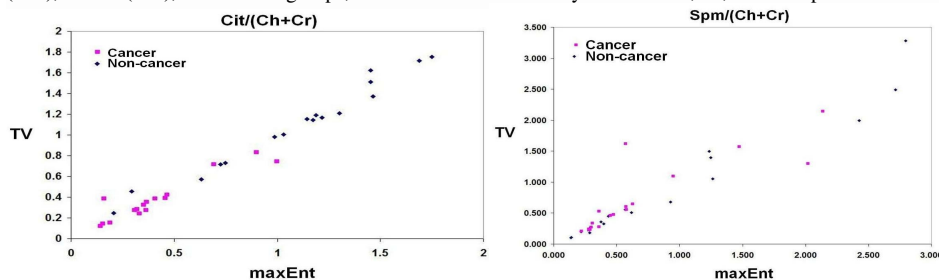


Figure 1. Correlation of MaxEnt-processed data with TV of Cit and Spm ratios

Metabolites wrt (Ch+Cr)	Cancer (Mean ± SD)	Non-Cancer (Mean ± SD)
maxEnt		
Cit	0.378±0.213	1.115±0.442
Spm	0.498±0.323	0.633±0.560
mI	0.189±0.119	0.232±0.146
TV		
Cit	0.413±0.252	1.108±0.449
Spm	0.505±0.319	0.918±0.817
mI	0.214±0.154	0.276±0.215

Table.1. Metabolites ratio of maxEnt and TV

Conclusion: We were able to detect and quantify metabolites using NUS based 4D EP-JRESI data acquired in clinically acceptable time (<12 minutes). We have shown that it possible to undersample the 4D EP-JRESI sequence with an acceleration factor of 4X and the data can be reliably reconstructed using TV and MaxEnt methods. Both non-linear reconstruction methods provide comparable results.

Acknowledgement: Authors acknowledge the support by an IDEA grant from the US Army Prostate Cancer Research Program: (#W81XWH-11-1-0248).

References: 1. American Cancer Society. Cancer Facts & Figures 2013. Atlanta, Ga: American Cancer Society; 2013. 2. Ryner LN, Sorenson JA, Thomas, MA. Magn. Reson. Imag. 1995; 13: 853–869. 3. Nagarajan R, Gomez AM, Raman SS, et al. NMR Biomed. 2010 Apr;23(3):257-61. 4. Lustig M, Donoho D, Pauly JM. Magn Reson Med. 2007 Dec;58(6):1182-95. 5. Furuyama JK, Wilson NE, Burns BL, et al. Magn Reson Med. 2012 Jun;67(6):1499-505. 6. Goldstein et al. SIAM J. Imaging Sci. 2009; 2: 323-343. 7. Hoch & Stern. NMR Data Processing, Wiley-Liss, New York, 1996. 8. Skilling & Bryan, Mon. Not. Roy. Astr. Soc. 1984; 211: 111-124.

MAXIMUM ENTROPY RECONSTRUCTED ECHO PLANAR BASED SPECTROSCOPIC IMAGING AND DIFFUSION WEIGHTED IMAGING IN PROSTATE CANCER

Rajakumar Nagarajan¹, Zohaib Iqbal¹, Brian Burns¹, Daniel A Margolis¹, Manoj K Sarma¹, Robert E Reiter², Steven S Raman¹, and M. Albert Thomas¹

¹Radiological Sciences, University of California Los Angeles, LOS ANGELES, CA, United States, ²Urology, University of California Los Angeles, LOS ANGELES, CA, United States

Introduction: In the United States, 90% of men with prostate cancer (PCa) are older than 60 years, diagnosed by early detection with the serum prostate-specific antigen (PSA) blood test, and have disease believed to be confined to the prostate gland (1). In vivo proton MRS provides biochemical information on the prostate tissues by providing relative concentrations of citrate (Cit), creatine (Cr), choline (Ch) and polyamines that are used to detect and diagnose PCa (2). The challenging task in 1D MRS spectra of PCa is the quantification of individual metabolites, due to spectral overlap of metabolites because of limited spectral dispersion at clinically used magnetic field strengths of less than 3T. Conventional phase encoded MRSI is relatively inefficient and time-consuming because it involves a large number of phase encodings. The applicability of compressed sensing (CS) (3) to four dimensional (4D) echo planar based J-Resolved spectroscopic imaging (EP-JRESI) in order to accelerate data acquisition using nonuniform under sampling (NUS) (4). This could be significantly reduced without sacrificing the spectral quality while maintaining high spatial resolution as well as the 4D EP-JRESI detect more metabolites (mI, glutamate, glutamine, spermine and lactate) compared to long TE conventional method. In this study maximum entropy (MaxEnt) method was used to reconstruct the 4D EP-JRESI data. Diffusion weighted imaging (DWI) has the ability to qualitatively and quantitatively represent the diffusion of water molecules by the apparent diffusion coefficient (ADC), which indirectly reflects tissue cellularity (5). The major goal of the study is to demonstrate the feasibility of correlating MaxEnt reconstructed 4D EP-JRESI data with DWI-MRI in PCa patients in 3T.

Materials and Methods: 4D EP-JRESI and DWI were recorded in eighteen PCa patients ranging in age from 46–73 years (mean, 65 years using Siemens 3T MRI Scanner (Siemens Medical Systems, Germany). This study was approved by the Institutional Review Board, and informed consent was obtained from each patient. The mean delay between biopsy and MRI was 8 weeks. A 4D NUS EP-JRESI sequence was implemented on a Siemens 3T Trio-Tim scanner and the volume of interest (VOI) was localized using three slice-selective radio-frequency (RF) pulses (90°-180°-180°). The CS-based reconstruction will enable a stable and accurate reconstruction from the NUS based EP-JRESI data (25% of t₁ and k_y increments) with a reduced total time. The parameters for the EPJRESI were: TR/TE/Avg = 1.5s/30ms/1-2, 16 phase encoding steps, 512 complex points with an F2 bandwidth of 1190Hz. For the second dimension (F1), 64 increments with bandwidths of 1000Hz were used. A 25% NUS was imposed along the incremented spectral and spatial dimensions. The individual voxel volume in human prostate was 1ml. MaxEnt is a constrained convex optimization algorithm that uses a variant of the conjugate gradient method to iteratively solve the inverse problem (6):

$$\text{maximize } S_{1/2}(f) \text{ s.t. } \|F^{-1} Kf - D\|_2 \leq \sigma \quad (1)$$

where f is the estimated fully-sampled spectrum at each iteration, F^{-1} is the inverse Fourier transform, K is the NUS matrix, D is the time-domain measured data, σ is the noise standard deviation, and $S_{1/2}(f)$ is the spin-1/2 entropy of the estimated spectrum (7). In addition, DWI-MRI was acquired with the following parameters: (TR/TE 3200/60 ms, bandwidth 1250 Hz in the EPI frequency direction) with b values of 0, 100, 400 and 800 s/mm².

Receiver operating characteristic (ROC) curve analyses based on logistic regression models were performed to predict the MRSI and ADC values. P values < 0.05 were considered statistically significant.

Results: Figure 1 show the ratios of myo-inositol (mI), spermine (Spm) and Cit with respect to Cr as well as (Ch+Cr). Fig.2 shows the ADC values between cancer and non-cancer locations of PCa patients. An investigation of the measurement of EP-JRESI with DWI data showed interesting results in this study. Since Ch and Cr are not always well resolved, adding to the uncertainty, we have calculated two different ratios (Cr, (Ch+Cr)). Table 1 shows the receiver operating characteristic (ROC) curve analyses based on logistic regression models were performed to predict the EP-JRESI and ADC values. Combining both EP-JRESI and ADC gives 100% accuracy in this selected group of patients. We have detected myo-inositol, glutamine, glutamate, spermine in addition to Cit, Cr and Ch. The NUS based 4D EP-JRESI data were processed using MATLAB based post processing. We have found significant (p<0.05) decrease of Cit, spm, with respect to (Ch+Cr) in cancer locations compared to non-cancer locations. Also decreased trend of mI was observed with respect to (Ch+Cr) ratio. Similar trends followed in Cr ratio except mI. However, because of the small number of samples in each group the differences in mI/Cr, mI/(Ch+Cr) did not reach statistical significance. The ROI based mean ADC values of cancer and non-cancer locations in the peripheral zones were: (0.985±0.164) and (1.453±0.168). The statistical significance (p <0.05) was observed between cancer and non-cancer locations.

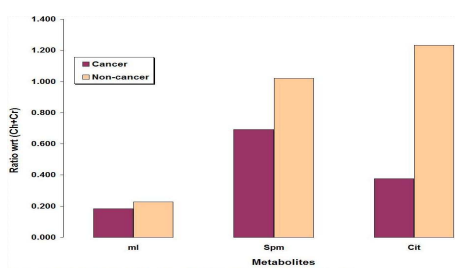


Fig 1. Metabolites ratios with respect to (Ch+Cr)

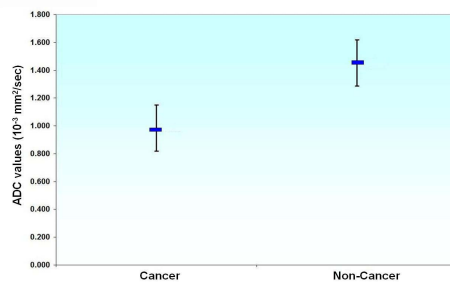


Fig 2. ADC values from Cancer and non-cancer

Parameter (%)	MRSI	ADC
Sensitivity	86.7	95.2
Specificity	95.5	95.0
PPV	91.3	94.3
NPV	92.8	93.0
Accuracy	91.5	93.1
AUC	97.0	97.4

Table.1. Findings from EP-JRESI and DWI

Discussion: Normal prostate epithelial cells produce and accumulate a large amount of Cit which is secreted as a major component of the prostatic fluid. Compared to normal tissue, decreased levels of Cit are previously observed in PCa tissue by ex vivo MRS (8). why ex vivo only Decrease in polyamines is associated with prostate cancer (9). Additionally, the very low putrescine concentration in our study confirms that the polyamine peak predominantly consists of Spm. Spm cannot be fully separated from the Ch peak using 1D spectral based MRSI, but with EP-JRESI we were able to detect and quantify nicely. The increase of mI/Cr was discussed in PCa earlier which agreed with our result (10) and decrease of mI/(Ch+Cr) may be due to the overlap of Ch and Cr which needs to be investigated in the future. The lower mean ADC values in the more aggressive tumors in our study may be due to higher cellular density in poorly differentiated tumors, resulting in more restricted movement of water protons (11).

Conclusion: It is evident from our preliminary investigation using a 3T MRI scanner that NUS based 4D EP-JRESI with MaxEnt reconstruction facilitates unambiguous detection of less T2-weighted metabolites compared to conventional 1D MRSI. DWI is potentially useful in PCa detection and localization. Our pilot findings demonstrate a possible clinical application of the 4D NUS EP-JRESI sequence in combination with DWI which may be useful in localizing PCa for diagnosis, monitoring, biopsy, treatment planning and staging as well as potentially for response assessment.

References:

- Jani AB, Johnstone PAS, Liauw SL, et al. American Journal of Clinical Oncology. 2008;31(4):375–378.
- Scheidler J, Hricak H, Vigneron DB, et al. Radiology 1999; 213: 473–480.
- Lustig M, Donoho D, Pauly JM. Magn Reson Med. 2007 Dec;58(6):1182–95.
- Furuyama JK, Wilson NE, Burns BL, et al. Magn Reson Med. 2012 Jun;67(6):1499–505.
- Gibbs P, Pickles MD, Turnbull LW. Invest. Radiol. 2006; 41: 185–188.
- Hoch & Stern. NMR Data Processing, Wiley-Liss, New York, 1996.
- Burns BL, Wilson N, Thomas MA. NMR Biomed 2013 (in press).
- Kurhanewicz J, Dahiya R, Macdonald JM, et al. Magn Reson Med. 1993 Feb;29(2):149–57.
- Nagarajan R, Gomez AM, Raman SS, et al. NMR Biomed. 2010 Apr;23(3):257–61.
- Swanson MS, Vigneron DB, James JK, et al. ISMRM, 2001, 2336.
- DeSouza NM, Reinsberg SA, Scurr ED, et al. Br J Radiol 2007; 80:90–95.

COMPRESSED SENSING BASED ECHO PLANAR 3D MRSI USING SHORT ECHO TIME: A PILOT EVALUATION USING A PROSTATE PHANTOM

Rajakumar Nagarajan¹, Neil Wilson¹, and M.Albert Thomas¹

¹Radiological Sciences, University of California Los Angeles, LOS ANGELES, CA, United States

Target audience: MR Physicist, Pulse sequence developers and Clinicians

Introduction: MRSI of the prostate is typically performed with a combination of point-resolved spectroscopy (PRESS) (1) volume localization and three dimensional (3D) MRSI (2) rather than the traditional single-voxel or two-dimensional (2D) MRSI technique used for many years in brain imaging. Three-dimensional MRSI requires phase encoding in three dimensions, conventionally known as frequency, phase, and slice. Acquisition time and coverage of the prostate are the main considerations in choosing the matrix dimensions. The MRSI data can be acquired with higher spatial resolution leading to long total acquisition time. Conventional prostate MRSI study with average weighted encoding uses long echo time (TE) with short repetition time (TR) allowing the observation of a reduced number of metabolites without accurate quantitation. Long TEs are used for the 3D MRSI due to the addition of MEGA radio-frequency pulses for both water and lipid suppression. In echo-planar spectroscopic imaging (EPSI) (3,4), an alternating gradient, which simultaneously encodes space and chemical shift (time), is applied along one of the spatial (readout) directions, thereby reducing phase encoding dimensions from three to two thereby increasing speed. MRI is well suited for compressed sensing (CS), and there are significant benefits in imaging speed and reduced costs, thereby improving patient care (5,6). A major challenge in designing CS data acquisition methods for MRI is in implementing non-uniform under sampling (NUS) densities that result in incoherent aliasing while providing data sparsity in a transform domain, such as wavelets, curvelets, etc. The goal of the present study was to implement a novel NUS based 3D EPSI on a 3T MRI/MRS scanner and to evaluate the performance using a prostate phantom.

Materials and Methods: A schematic diagram of NUS based 3D EPSI sequence, compiled and implemented on the Siemens 3T MRS scanner, is shown in Figure 1 where three spatial encodings and one spectral dimension were used. In the 3D EPSI sequence, the EPSI readout simultaneously acquires one spatially encoded dimension (k_x) and one spectral dimension (t), leaving the remaining the two spatial dimensions (k_y and k_z , respectively) incremented sequentially. We propose the use of NUS in the remaining k_y - k_z plane, using CS to reconstruct the equivalent missing data to a fully sampled 3D EPSI acquisition.

To determine the feasibility as well as to evaluate the performance of the CS reconstruction, numerous prospective 2X undersampling and reconstructions were performed on a prostate 3D EPSI of nine phantom dataset and two healthy volunteers using external phased array coil. A 500mL prostate phantom was prepared containing the following metabolites at physiological concentrations as reported in healthy human prostate (7): Cit, 50 mM, Cr, 5 mM, Ch, 1 mM, Spm, 6 mM, mI, 10 mM, PCh, 2 mM, Tau, 3 mM, Glu, 4 mM, Gln, 2.5mM and sI, 0.8 mM. The dataset was localized with a field of view (FOV) of 24x24x16 cm³ for an individual voxel volume of 1.5 cm³; 256 bipolar gradient echo pairs (t samples) were collected with bandwidth of 1190 Hz. A non-water-suppressed 3D EPSI data using one average was used for eddy current and phase correction of the suppressed data. With pulse repetition time/echo time = 1500/30 ms and 8 averages, the 3D EPSI phantom scan duration was 12 minutes. Global water suppression was performed just before the PRESS localization.

Results: Both the non-water suppressed (NWS) and water suppressed (WS) scans were separated into positive (even) and negative (odd) subsets first and reorganized into k_x - k_y - k_z - t matrices. Reconstruction of the NUS based 3D EPSI data sets was done offline using a custom MATLAB software package. Fig.2. shows the extracted 1D spectrum from the central voxel from the prostate phantom (volume of 1cm³). We were able to detect and quantitate glutamate/glutamine (Glx), spermine, myo-inositol in addition to citrate, choline and creatine. The metabolite quantitation was done by Felix peak integral quantitation method. The mean and standard deviation of metabolites with respect to creatine were: Citrate (12.642±3.230), spermine ((1.108±0.167), choline (0.619±0.069), myo-inositol (1.816±0.345) and Glx (2.239±0.267). The expected and calculated experimental metabolite ratios with respect to creatine are shown in Fig.3.

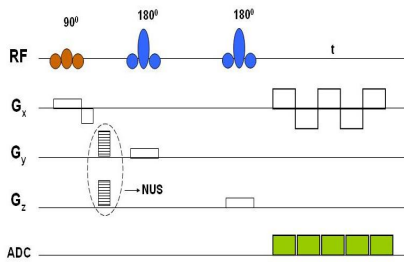


Fig.1. NUS based 3D EPSI sequence

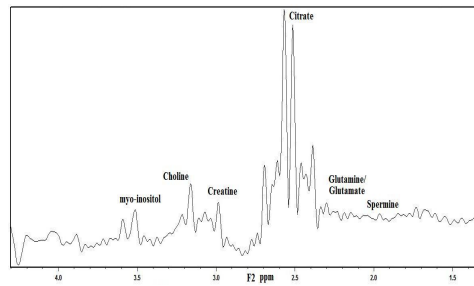


Fig.2. An extracted spectrum from the central voxel

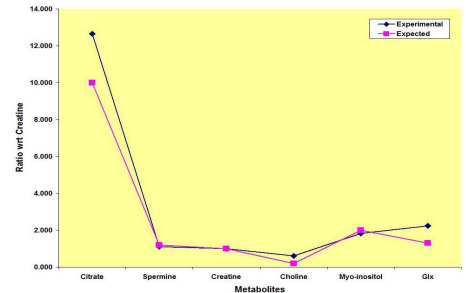


Fig.3. Comparison of experimental and expected metabolites ratios wrt creatine

Discussion: By using CS based reconstruction, we have demonstrated a potential reduction in acquisition time by up to 80% for proton MRSI, with negligible loss of information as evaluated on the basis of clinically relevant metrics. The NUS 3D spatial +1D spectral encoded EPSI sequence recorded short TE-based spectra from multiple regions of a prostate phantom and showed more metabolites in addition to the normally detected citrate, creatine, choline and spermine.

Conclusion: The NUS based 3D EPSI data using CS reconstruction to detect and quantify metabolites less T2-weighted than the earlier 3D MRSI sequences using conventional phase encoding. It could be employed to help detect prostate cancer more accurately thereby eradicating negative biopsies, evaluate cancer stage noninvasively, and guide treatment selection. Our current effort is focused on developing an optimal sequence with interleaved water-suppressed metabolite and unsuppressed water acquisition.

References:

1. Bottomley PA. Ann N Y Acad Sci. 1987;508:333-48.
2. Brown TR, Kincaid BM, Ugurbil K. Proc Natl Acad Sci USA 1982 ; 79:3523–3526.
3. Mansfield P. Magn Reson Med 1984; 1(3): 370–386.
4. Posse S, Tedeschi G, Risinger R, et al. MRM (1995): 34-40.
5. Donoho D. IEEE Trans Info Theory 2006;52:1289-1306.
6. Lustig M, Donoho D, Pauly JM. Magn Reson Med. 2007;58(6):1182-95.
7. Lange T, Schulte RF, Boesiger P. Magn Reson Med. 2008 May;59(5):966-72.



Accelerated Echo Planar J-Resolved Spectroscopic Imaging in Prostate Cancer: Nonlinear Reconstruction Using Total Variation And Maximum Entropy

Journal:	<i>NMR in Biomedicine</i>
Manuscript ID:	NBM-14-0247
Wiley - Manuscript type:	Research Article
Date Submitted by the Author:	10-Sep-2014
Complete List of Authors:	Nagarajan, Rajakumar; University of California, Los Angeles, Department of Radiological Sciences Iqbal, Zohaib; University of California, Los Angeles, Department of Radiological Sciences Burns, Brian; University of California, Los Angeles, Department of Radiological Sciences Wilson, Neil; University of California, Los Angeles, Department of Radiological Sciences Sarma, Manoj; University of California, Los Angeles, Department of Radiological Sciences Margolis, Daniel; University of California, Los Angeles, Department of Radiological Sciences Reiter, Robert; University of California, Los Angeles, Urology Raman, Steve; University of California, Los Angeles, Department of Radiological Sciences Thomas, Michael; University of California, Los Angeles, Department of Radiological Sciences
Keywords:	Acquisition Methods < Methods and Engineering, Compressed sensing < Acquisition Methods < Methods and Engineering, MR Spectroscopy (MRS) and Spectroscopic Imaging (MRSI) Methods < Methods and Engineering

SCHOLARONE™
Manuscripts

1
2
3
4
5
6
7
8
9
10
11
12
13
14
15
16
17
18
19
20
21
22
23
24
25
26
27
28
29
30
31
32
33
34
35
36
37
38
39
40
41
42
43
44
45
46
47
48
49
50
51
52
53
54
55
56
57
58
59
60

Accelerated Echo Planar J-Resolved Spectroscopic Imaging in Prostate Cancer: Nonlinear Reconstruction Using Total Variation And Maximum Entropy

Rajakumar Nagarajan^a, Zohaib Iqbal^a, Brian Burns^a, Neil Wilson^a, Manoj K Sarma^a, Daniel A Margolis^a, Robert E Reiter^b, Steven S Raman^a, and M. Albert Thomas^a

^a*Radiological Sciences, University of California Los Angeles, Los Angeles, CA, United States,*

^b*Urology, University of California Los Angeles, Los Angeles, CA, United States*

Running Title: Fast MR Spectroscopic Imaging of Prostate Cancer

*** Correspondence:**

M. Albert Thomas Ph.D

Radiological Sciences

David Geffen School of Medicine at UCLA

Tel: (310) 206 4191 Fax: (310) 825 5837

Email: athomas@mednet.ucla.edu

Abstract

Overlap of metabolites is a major limitation in one-dimensional (1D) spectral-based single voxel MR Spectroscopy (MRS) and multivoxel-based MR spectroscopic imaging (MRSI). By combining echo-planar spectroscopic imaging (EPSI) with two-dimensional (2D) J resolved spectroscopic sequence (JPRESS), 2D spectra can be recorded in multiple locations in a single slice of prostate using four dimensional (4D) Echo-Planar J-Resolved Spectroscopic Imaging (EP-JRESI) combining 2 spectral with 2 spatial dimensions. The goal of the present work was to investigate metabolite levels after non-linear reconstruction of an accelerated 4D EP-JRESI data using Maximum Entropy (MaxEnt) and Total Variation (TV) in Prostate Cancer (PCa). Twenty two prostate cancer patients with a mean age of 63.8 years (range: 46–79 years) were investigated in this study. A 4D non-uniformly under-sampling (NUS) EP-JRESI sequence was implemented on the Siemens 3T MRI scanner. The NUS data was reconstructed using two non-linear reconstruction methods, namely MaxEnt and TV. Significant decrease of Cit in cancer locations and decreased levels of Spermine (Spm), myo-Inositol (mI), and increased levels of Glutamate and Glutamine (Glx) with respect (Choline (Ch)+Creatine (Cr)) were observed in cancer locations compared to non-cancerous tissues when the acquired 4D EP-JRESI data was reconstructed using TV and MaxEnt. We have shown that it is possible to accelerate the 4D EP-JRESI sequence by 4X and the data can be reliably reconstructed using the TV and MaxEnt methods. The total acquisition duration was less than 13 minutes and we were able to detect and quantify several metabolites.

1
2
3 **KEYWORDS:** Magnetic Resonance Spectroscopy, Prostate Cancer, 4D EP-JRESI,
4
5 Citrate, Myo-inositol, Glx, Echo planar spectroscopic imaging.
6
7

8
9
10 **Abbreviations used:** PCa, prostate cancer; PSA, prostate specific antigen; DRE, digital
11
12 rectal examination; MaxEnt, maximum entropy; TV, total variation; NUS, non-uniform
13
14 undersampling; VOI, volume of interest; ROC, receiver operating charecterstic; PPV,
15
16 positive predictive value; NPV, negative predictive value; MRSI, magnetic resonance
17
18 spectroscopic imaging; CS, compressed sensing; JPRESS, J-resolved spectroscopy; Ch,
19
20 choline; Cr, creatine; Cit, citrate; Spm, spermine; mI, myo-inositol; Glu, glutamate; Gln,
21
22 glutamine; 1D, one-dimensional; 2D, two-dimensional; 3D, three-dimensional; 4D, four-
23
24 dimensional; RF, radio-frequency; SNR, signal to noise ratio; EPSI, echo planar
25
26 spectroscopic imaging; EP-JRESI, echo-planar J-resolved spectroscopic imaging;
27
28
29
30
31
32
33
34
35
36
37
38
39
40
41
42
43
44
45
46
47
48
49
50
51
52
53
54
55
56
57
58
59
60

Introduction

Prostate cancer (PCa) is the most commonly diagnosed noncutaneous malignancy in the USA and is the second-leading cause of cancer-related death in men (1). One in 6 men will be diagnosed with PCa during his lifetime but only one in 36 will die of this disease. Currently, annual prostate specific antigen (PSA) test and digital rectal examination (DRE) are routinely performed (2) for screening. PSA is a controversial screening test that measures the serum level of PSA in blood samples, as 65–75 % of PSA screening gives false-positive results leading to over-diagnosis (3). The use of systematic transrectal biopsy can miss significant prostate cancers, because of both a random sampling error (4), and because up to a third of significant tumors lie in the anterior part of the gland, based on studies of radical prostatectomy specimens (5). Hence, there is an immediate need for early yet accurate detection of PCa to improve disease outcomes.

Proton MR Spectroscopy (^1H -MRS) enables detecting a range of biochemicals in prostate by making use of the proton signals in these molecules. Detection of biochemicals in vivo is limited to concentrations of more than 0.5–1 mM. Signals of citrate (Cit), creatine (Cr), choline (Ch) and spermine (Spm) can be detected throughout the prostate, with increased levels of Ch and decreased levels of Cit being indicative of cancer (6-8).

Current limitations of single voxel based MRS and MR spectroscopic imaging (MRSI) in prostate is due to the overlap of metabolite resonances, allowing the quantification of only a few metabolites (Cit, Ch, Cr and Spm) and use of long echo times. The conventional MRSI technique can be accelerated by echo-planar spectroscopic imaging (EPSI) (9-13). The EPSI speeds up MRSI by using an echo-planar read-out of

1
2
3 one spectral and one spatial dimensions, thereby achieving an acceleration factor equal to
4 the number of points along one of spatial dimensions. For example, in a 2D spatial matrix
5 array (16*16) would take 16 times less time with EPSI than the conventional MRSI.
6
7
8 However, the acceleration may be at the cost of signal to noise ratio (SNR) (14) and
9 spectra could be affected by Nyquist ghost artifacts (15).
10
11
12
13

14
15 A single-voxel based 2D JPRESS has been evaluated in PCa, and showed
16 improved spectral dispersion due to the added spectral dimension (16,17). Compressed
17 sensing was recently introduced as a powerful method to accelerate MRI by exploiting
18 the sparsity of the images in a known transform domain to reconstruct non-uniformly
19 undersampled (NUS) k-space data (18). By combining EPSI with JPRESS, 2D spectra
20 can be recorded in multiple locations in prostate using four dimensional (4D) Echo-
21 Planar J-Resolved Spectroscopic Imaging (EP-JRESI) combining 2 spectral with 2 spatial
22 dimensions. A pilot feasibility was demonstrated recently to map metabolites in the
23 healthy human prostate and brain (19, 20).
24
25
26
27
28
29
30
31
32
33
34
35

36 The Maximum Entropy method (MaxEnt) has proved to be an enormously
37 powerful tool for reconstructing images from many types of MRI data but it has been
38 used most spectacularly in astronomy, where it deals routinely with images of up to a
39 million pixels, with high dynamic range (21). Maximum entropy and total variation (TV)
40 algorithms have been used to reconstruct NUS indirect spectral and spatial dimensions
41 (22).
42
43
44
45
46
47
48
49

50 The TV algorithm was first proposed by Rudin et al. (23) for image denoising and
51 since then has been successfully used for image restoration. In the TV algorithm, an
52 objective function using the TV norm is minimized subject to a data fidelity posed by the
53
54
55
56
57
58
59
60

1
2
3 acquired projection data. Minimizing the image gradient essentially suppresses those high
4
5 spatial frequency parts such as streaking artifacts and noise in the reconstructed images.
6
7

8 The goal of the present work was to compare MaxEnt and TV reconstruction of
9
10 the accelerated 4D EP-JRESI data acquired in PCa patients.
11
12

13 **Materials and Methods**

14
15
16 **Patients:** Between March 2012 and May 2013, twenty two PCa patients with a mean age
17
18 of 63.8 years (range: 46–79 years) who underwent radical prostatectomy were selected
19
20 for the study. Patients' Gleason scores varied between 6 and 9. Prostate-specific antigen
21
22 (PSA) varied from 0.7 to 22.8 ng/mL (mean of 6.23 ng/mL). These patients were scanned
23
24 using a 3T Siemens (Siemens Medical Solution, Erlangen, Germany) MRI scanner with
25
26 an endorectal "receive" coil. The protocol combining MRI and MRS was performed at
27
28 least 8 weeks after transrectal ultrasound-guided sextant biopsy. The entire protocol was
29
30 approved by the Institutional Review Board, and informed consent was obtained from
31
32 each patient. Prostate cancer was histopathologically confirmed and graded after radical
33
34 prostatectomy. The voxels covering the tumorous lesions from the peripheral zone (PZ)
35
36 were selected and indicated as tumor voxels. After reconstruction the EP-JRESI were
37
38 overlaid onto MRI images.
39
40
41
42
43
44
45

46
47 **MRI and MRSI:** A combined body matrix phased-array coil assembly and an endorectal
48
49 coil were used in the "receive" mode while a quadrature body coil was used for
50
51 "transmit". All patients were imaged in supine feet-first position. Axial images were
52
53 oriented to be perpendicular to the long axis of the prostate, which was guided by the
54
55 sagittal images. Axial, coronal, and sagittal T₂-weighted (T₂W) turbo spin-echo imaging
56
57
58
59
60

was performed with the following parameters: repetition time/echo time (TR/TE), 3850–4200/96–101 ms; section thickness, 3 mm; field of view, $20 \times 20 \text{ cm}^2$; echo train length, 13; matrix, 320×256 .

A 4D NUS EP-JRESI sequence was implemented on the 3T MRI scanner and the volume of interest (VOI) was localized using three slice-selective radio-frequency (RF) pulses (90° - 180° - 180°) (Fig.1). The total time for obtaining a fully sampled 4D EP-JRESI scan (TR of 1.5s, $16k_y * 16k_x$, 64 - $100t_1$, $512t_2$) can be more than 25 minutes. The parameters for the EP-JRESI were: TR/TE/Avg = 1500/30ms/1-2, 16 phase encoding steps, 512 complex points with an F_2 bandwidth of 1190Hz. For the second dimension (F_1), 64 increments with bandwidths of 1000Hz were used. A 4X NUS was imposed along the plane containing incremented spectral and spatial dimensions (t_1 and k_y). The individual voxel volume in human prostate was 1ml. Two sets of data were collected, one water suppressed scan (WS) with a total scan time of 6-12 minutes and a second non-water suppressed scan (NWS) using one average only.

Data Analysis: The NUS data were reconstructed by MaxEnt and TV separately. A modified Split-Bregman algorithm (21) solves the unconstrained TV optimization problem as shown in Eqn.(1) below:

$$\min_m \|\nabla m\|_1 + \lambda \|F_u m - y\|_2 \quad (1)$$

where ∇ is the gradient operator, m is the reconstructed data, $\|x\|_1$ is the l_1 -norm, λ is a regularization parameter, F_u is the under sampled Fourier transform, and y is the under-sampled data. The above equation removes the incoherent artifacts due to NUS by

1
2
3 minimizing the total variation (TV) while maintaining consistency with the sampled
4
5 measurements.
6

7
8 MaxEnt is a constrained convex optimization algorithm that uses a variant of the
9
10 conjugate gradient method to iteratively solve the inverse problem (21, 24, 25):
11

$$12 \quad \text{maximize } S_{1/2}(f) \text{ s.t. } \|F^{-1} Kf - D\|_2 \leq \sigma \quad (2)$$

13
14 where f is the estimated fully-sampled spectrum at each iteration, F^{-1} is the inverse
15
16 Fourier transform, K is the NUS matrix, D is the measured time-domain data, σ is the
17
18 noise standard deviation, and $S_{1/2}(f)$ is the spin- $1/2$ entropy of the estimated spectrum (26).
19

20 All NUS based 4D EP-JRESI data were processed using TV and MaxEnt reconstruction
21
22 with custom MATLAB software.
23
24
25
26
27

28 29 **Statistical Analysis:**

30
31 Statistical analyses were performed with SPSS 21 (SPSS Inc., Chicago, IL, USA). Using
32
33 logistic regression analysis, areas under the curve (AUC) of the receiver operating
34
35 characteristic (ROC) were calculated for various metabolites in discriminating between
36
37 MaxEnt and TV reconstruction methods. Also the paired t-test was used to determine the
38
39 various metabolite ratios in cancer and non-cancer locations. A p-value less than 0.05
40
41 was considered statistically significant.
42
43
44
45
46

47 48 **Results**

49
50 We were able to detect Cit, Ch, Cr, Spm, myo-inositol (mI), and glutamate plus
51
52 glutamine (Glx) in cancer and non-cancer locations and quantified using the peak
53
54 integration method. Figs. 2 and 3 show the metabolite ratios of Cit, Spm, mI, and Glx of
55
56 cancer and non-cancer locations processed by MaxEnt and TV. The mean metabolite
57
58
59
60

1
2
3 ratios and standard deviations (SD) of Cit, Spm, mI and Glx with respect to (Ch+Cr)
4
5 were quantified for the TV reconstructed non-cancer locations as: 1.215 ± 0.537 , 0.801
6
7 ± 0.622 , 0.214 ± 0.106 , 0.228 ± 0.105 . In the cancer location, the metabolites ratios were:
8
9 0.361 ± 0.241 , 0.607 ± 0.457 , 0.202 ± 0.073 , 0.246 ± 0.146 . Similarly the mean metabolite
10
11 ratios and SD of Cit, Spm, mI and Glx with respect to (Ch+Cr) were quantified for the
12
13 MaxEnt reconstructed non-cancer locations as: 1.234 ± 0.557 , 0.929 ± 0.629 , 0.238 ± 0.101 ,
14
15 0.219 ± 0.105 . In the cancer locations, the metabolite ratios were: 0.347 ± 0.188 , 0.581
16
17 ± 0.335 , 0.210 ± 0.144 , 0.234 ± 0.175 .

18
19
20
21
22 We found that mean Cit metabolite ratios were significantly lower in cancer locations
23
24 compared to non-cancerous locations in both TV and MaxEnt reconstruction. Decreased
25
26 levels of Spm, mI and increased levels of Glx with respect to (Ch+Cr) ratio were
27
28 observed in cancer locations compared to non-cancer locations in the TV and MaxEnt
29
30 reconstructions. There were no statistically significant changes when metabolites ratio
31
32 were correlated with GS.
33
34

35
36 Fig.4 shows a spatial maps of (Ch+Cr) for the TV and MaxEnt reconstructed data
37
38 acquired in a 74 year old PCa patient. The MaxEnt and TV reconstructions of cancer
39
40 (B&D) and non-cancer (C&E) locations extracted from the JPRESS spectrum of a 4D
41
42 EP-JRESI voxel is shown in Fig.5. We have compared and correlated the TV with
43
44 MaxEnt reconstruction methods of Cit, Spm, mI and Glx in the cancer and non-cancer
45
46 locations. The correlation of the Cit/(Ch+Cr), Spm/(Ch+Cr), mI/(Ch+Cr) and
47
48 Glx/(Ch+Cr) ratios for the MaxEnt and TV reconstructions in cancer and non-cancer
49
50 locations are shown in Fig.6. A positive correlation was found in the following
51
52 metabolites in cancer locations: Cit/(Ch+Cr) ($R^2=0.963$), Glx/(Ch+Cr) ($R^2=0.918$),
53
54
55
56
57
58
59
60

1
2
3 Spm/(Ch+Cr) ($R^2=0.905$) and mI/(Ch+Cr) ($R^2=0.820$). Also we observed positive
4
5 correlation of the above mentioned metabolites in non-cancer location (not reported).
6
7

8 Detailed results of the logistic regression analysis and consequent receiver
9
10 operating characteristic (ROC) curve analyses are given in Table 1 including the
11
12 sensitivity, specificity, positive predictive value (PPV), negative predictive value (NPV),
13
14 area under curve (AUC), and accuracy for classifying the MaxEnt and TV methods. ROC
15
16 curve analyses for differentiating the metabolite ratios of cancer and non-cancer locations
17
18 in MaxEnt suggest Cit gives the best predictability with sensitivity 86.4%, specificity
19
20 86.4%, accuracy 86.4% and AUC 94.0%. Also the overall sensitivity, accuracy and AUC
21
22 of mI and Spm were slightly higher in MaxEnt compared to TV.
23
24
25
26
27
28

29 Discussion

30
31 Using NUS with non-linear iterative reconstruction, we have demonstrated a potential
32
33 reduction of acquisition times by up to 75% for EP-JRESI with minimal loss of
34
35 information. In addition to significant decrease of Cit in cancer locations, decreased
36
37 metabolite ratios of Spm, mI and increased Glx were found in cancer locations compared
38
39 to non-cancer locations. Even though TV and MaxEnt reconstruction showed comparable
40
41 results in cancer and non-cancer locations, there was a slight increase of sensitivity,
42
43 accuracy and AUC in MaxEnt reconstruction.
44
45
46
47

48 In the present study, we report the relative concentrations of Cit, Spm, mI and Glx
49
50 with respect to (Ch+Cr), because the total Cr peak (3.0 ppm) is very close to the total Ch
51
52 peak (3.2 ppm) in these *in vivo* MR spectra and may not always be separable. In this
53
54 study, significantly higher level of Cit was observed in the peripheral zone of healthy
55
56
57
58
59
60

1
2
3 prostates. The production and storage of citrate is one of the main characteristics of
4
5 normal prostate.
6

7
8 It is likely that the drop in Cit precedes malignant transformation (27). It has been
9
10 suggested that, due to a metabolic switch, neoplastic cells would become Cit oxidizing,
11
12 unlike normal prostatic cells that show a low Cit-oxidizing capability (28). Decreased
13
14 levels of zinc, which would relieve m-aconitase from inhibition, has been proposed as
15
16 one of the reasons for the decreased level of Cit in PCa (27).
17
18

19
20 Choline is an essential component of cell membrane synthesis and phospholipid
21
22 metabolism and functions as an important methyl donor. Choline-containing molecules
23
24 are an essential component of cell membranes, which are more highly concentrated in
25
26 tumorous areas within the prostate than in healthy prostate tissue. (29,30). Choline groups
27
28 are precursors and breakdown products of the phospholipid phosphatidylcholine, a major
29
30 cell membrane compound (31). Increased Ch is observed due to an altered phospholipid
31
32 metabolism in PCa cell lines (30). This alteration is most likely due to an increased
33
34 expression and activity of choline-kinase, a higher rate of choline transport, and an
35
36 increased phospholipase activity (31).
37
38
39

40
41 The polyamines spermine, spermidine, and putrescine are essential for the
42
43 differentiation and proliferation of cells, the synthesis of DNA, RNA, and proteins, and
44
45 the stabilization of cell membranes and cytoskeletal structures (32). Previous studies
46
47 observed high levels of spermine in healthy prostate tissue and BPH and reduced
48
49 spermine levels in malignant prostate tissue (17, 33-35).
50
51

52
53 The osmoregulator myo-inositol is expressed in a variety of tissues, and its
54
55 decrease was observed in PCa within human expressed prostatic secretions (EPS) using
56
57
58
59
60

1
2
3 high resolution NMR (36) and in breast tumors (37). In our study, slightly decreased ml
4
5 were observed in cancer locations but were not statistically significant.
6
7

8 Glu and Gln are difficult to be resolved, owing to the overlap of resonances. As a
9
10 result, most reliable MRS studies use the sum of Glu and Gln (expressed as either Glx or
11
12 Glu + Gln). Glutamate is extensively involved in metabolic and oncogenic pathways.
13
14 Koochekpour (38) showed that serum glutamate levels directly correlated with Gleason
15
16 scores (<6 vs. >8) and primary PCa aggressiveness. In our study, elevations of Glx were
17
18 found in the cancer locations but were not statistically significant.
19
20
21

22 There was an overlap between cancer and non-cancer locations, possibly due to
23
24 the low signal-to-noise ratio of the Cr peak. In addition, Ch and Cr were not always well
25
26 resolved especially in cancer locations, adding to the uncertainty in quantitation.
27
28 However, using prior knowledge fitting (ProFit), accurate quantitation of metabolites can
29
30 be improved (39). Due to the small patient population, we did not find any significant
31
32 changes in other metabolites. Also this study focused in the peripheral zone of the
33
34 prostate where 80% of cancer occurs. The advantage of NUS based 4D EP-JRESI
35
36 sequence is in recording short TE-based spectra from multiple regions of human prostate
37
38 and more metabolites, such as myo-inositol, spermine and Glx in addition to the normally
39
40 detected citrate, creatine and choline.
41
42
43
44
45
46

47 **Conclusion**

48
49 We were able to detect metabolites using NUS based 4D EP-JRESI data acquired in
50
51 clinically acceptable times (<12 minutes). We have shown that it possible to undersample
52
53 the 4D EP-JRESI sequence with an acceleration factor of 4X and the data can be reliably
54
55
56
57
58
59
60

1
2
3 reconstructed using the TV and MaxEnt methods. Both non-linear reconstruction
4
5 methods provided comparable results.
6
7
8
9
10
11
12
13
14
15
16

17
18 **Acknowledgement:**

19
20 This work was supported by an CDMRP grant from the US Army Prostate Cancer
21
22 Research Program: (#W81XWH-11-1-0248).
23
24
25
26
27
28
29
30
31
32
33
34
35
36
37
38
39
40
41
42
43
44
45
46
47
48
49
50
51
52
53
54
55
56
57
58
59
60

References:

1. Siegel R, Naishadham D, Jemal A. Cancer statistics, 2013. *CA Cancer J Clin*. 2013 Jan;63(1):11-30.
2. Andriole GL, Crawford ED, Grubb RL 3rd, Buys SS, et al. Mortality results from a randomized prostate-cancer screening trial. *N Engl J Med* 2009; 360, 1310–1319.
3. Smith DS, Humphrey PA, Catalona WJ. The early detection of prostate carcinoma with prostate specific antigen: the Washington University experience. *Cancer* 1997; 80:1852–1856.
4. Djavan B, Ravery V, Zlotta A, Dobronski P, Dobrovits M, Fakhari M, Seitz C, Susani M, Borkowski A, Boccon-Gibod L, Schulman CC, Marberger M. Prospective evaluation of prostate cancer detected on biopsies 1, 2, 3 and 4: when should we stop? *J Urol* 2001; 166 :1679–1683.
5. McNeal JE, Redwine EA, Freiha FS, Stamey TA. Zonal distribution of prostatic adenocarcinoma. Correlation with histologic pattern and direction of spread *Am J Surg Pathol* 1988; 12; 897–906.
6. Thomas MA, Narayan P, Kurhanewicz J, Jajodia P, Weiner MW. 1H MR spectroscopy of normal and malignant human prostates in vivo. *J Magn Reson B* 1990;87:610–619.
7. Kurhanewicz J, Vigneron DB, Nelson SJ, Hricak H, MacDonald JM, Konety B, Narayan P. Citrate as an in vivo marker to discriminate prostate cancer from benign prostatic hyperplasia and normal prostate peripheral zone: detection via localized proton spectroscopy. *Urology* 1995;45:459–466.
8. Kurhanewicz J, Vigneron DB, Hricak H, Narayan P, Carroll P, Nelson SJ. Three-dimensional H-1 MR spectroscopic imaging of the in situ human prostate with high (0.24-0.7-cm³) spatial resolution. *Radiology* 1996;198:795–805.
9. Mansfield P. Spatial mapping of the chemical shift in NMR. *Magn Reson Med* 1994; 1: 370–386.
10. Matsui S, Sekihara K, Kohno H. High-speed spatially resolved high-resolution NMR spectroscopy. *J Am Chem Soc* 1985; 107: 2817–2818.
11. Posse S, Tedeschi G, Risinger R, Ogg R, Bihan DL. High speed 1H spectroscopic imaging in human brain by echo planar spatial-spectral encoding. *Magn Reson Med* 1995; 33: 34–40.
12. Ericsson A, Weis J, Sperber GO, Hemmingsson A. Measurements of magnetic field variations in the human brain using a 3D-FT multiple gradient echo technique. *Magn Reson Med* 1995; 33: 171–177.

- 1
2
3
4
5 13. Ebel A, Soher BJ, Maudsley AA. Assessment of 3D proton MR echo-planar
6 spectroscopic imaging using automated spectral analysis. *Magn Reson Med* 2001; 46:
7 1072–1078.
8
- 9 14. Posse S, Tedeschi G, Risinger R, Ogg R, Bihan DL. High Speed 1H Spectroscopic
10 Imaging in Human Brain by Echo Planar Spatial - Spectral Encoding. *Magn Reson Med*
11 1995; 33(1), 34-40.
12
- 13 15. Du W, Du YP, Fan X, Zamora MA, Karczmar GS. Reduction of spectral ghost
14 artifacts in high-resolution echo-planar spectroscopic imaging of water and fat resonances.
15 *Magn Reson Med* 2003;49(6):1113-1120.
16
17
- 18 16. Ryner LN, Sorenson JA, Thomas MA. Localized 2D J-resolved 1H MR spectroscopy:
19 strong coupling effects in vitro and in vivo. *Magn Reson Imaging* 1995;13(6):853-69.
20
21
- 22 17. Nagarajan R, Gomez AM, Raman SS, Margolis DJ, McClure T, Thomas MA.
23 Correlation of endorectal 2D JPRESS findings with pathological Gleason scores in
24 prostate cancer patients. *NMR Biomed* 2010 Apr;23(3):257-61.
25
26
- 27 18. Lustig M, Donoho D, Pauly JM. Sparse MRI: The application of compressed sensing
28 for rapid MR imaging. *Magn Reson Med* 2007 Dec;58(6):1182-95.
29
30
- 31 19. Furuyama JK, Wilson NE, Burns BL, Nagarajan R, Margolis DJ, Thomas MA.
32 Application of compressed sensing to multidimensional spectroscopic imaging in human
33 prostate. *Magn Reson Med* 2012 Jun;67(6):1499-505.
34
- 35 20. Sarma MK, Nagarajan R, Macey PM. Accelerated Echo-Planar J-Resolved
36 Spectroscopic Imaging in the Human Brain using Compressed Sensing: A Pilot
37 Validation in Obstructive Sleep Apnea. *AJNR Am J Neuroradiol* 2014; Jun;35(6
38 Suppl):S81-9.
39
40
- 41 21. Goldstein T and Osher S. The Split Bregman Method for L1 Regularized Problems.
42 *SIAM J. Imaging Sci* 2009; 2: 323-343.
43
44
- 45 22. Burns B, Wilson NE, Furuyama JK, Thomas MA. Non-uniformly under-sampled
46 multi-dimensional spectroscopic imaging in vivo: maximum entropy versus compressed
47 sensing reconstruction. *NMR Biomed* 2014;191-201.
48
- 49 23. Rudin L, Osher S, and Fatemi E. Nonlinear total variation based noise removal
50 algorithms. *Physica. D* 1992, 60:259-268.
51
52
- 53 24. Hoch CJ, Stern AS. *NMR Data Processing*, Wiley-Liss, New York, 1996.
54
- 55 25. Skilling J and Bryan RK. Maximum entropy image reconstruction: general algorithm,
56 *Monthly Notices of the Royal Astronomical Society* 1984; 211, 111-124.
57
58
59
60

- 1
2
3
4
5 26. Daniell GJ, Hore PJ. Maximum entropy and NMR—a new approach. *J Magn Reson* 1989; 4(3): 515–536.
6
7
8 27. Costello LC, Franklin RB. The intermediary metabolism of the prostate: a key to
9 understanding the pathogenesis and progression of prostate malignancy. *Oncology* 2000;
10 59: 269–282.
11
12 28. Costello LC, Franklin RB, Narayan P. Citrate in the diagnosis of prostate cancer.
13 *Prostate* 1999; 38: 237–245.
14
15 29. Kurhanewicz J, Swanson MG, Nelson SJ, Vigneron DB. Combined magnetic
16 resonance imaging and spectroscopic imaging approach to molecular imaging of prostate
17 cancer. *J Magn Reson Imaging*. 2002 Oct;16(4):451-63.
18
19 30. Ackerstaff E, Pflug BR, Nelson JB, Bhujwala ZM. Detection of increased choline
20 compounds with proton nuclear magnetic resonance spectroscopy subsequent to
21 malignant transformation of human prostatic epithelial cells. *Cancer Res* 2001;61:3599–
22 3603.
23
24 31. Glunde K, Bhujwala ZM. Metabolic tumor imaging using magnetic resonance
25 spectroscopy. *Semin Oncol* 2011;38:26–41.
26
27 32. Jänne J, Pösöo H, Raina A. Polyamines in rapid growth and cancer. *Biochim.*
28 *Biophys. Acta* 1978; 473: 241-293.
29
30 33. Van der Graaf M, Schipper RG, Oosterhof GO, Schalken JA, Verhofstad AA,
31 Heerschap A. Proton MR spectroscopy of prostatic tissue focused on the detection of
32 spermine, a possible biomarker of malignant behavior in prostate cancer. *MAGMA*
33 2000;10:153–9.
34
35 34. Thomas MA, Nagarajan R, Huda A, Margolis D, Sarma MK, Sheng K, Reiter RE,
36 Raman SS. Multidimensional MR spectroscopic imaging of prostate cancer in vivo.
37 *NMR Biomed* 2014 Jan;27(1):53-66.
38
39 35. Yue K, Marumoto A, Binesh N, Thomas MA. 2D JPRESS of human prostates using
40 an endorectal receiver coil. *Magn Reson Med* 2002 Jun;47(6):1059-64.
41
42 36. Serkova NJ, Gamito EJ, Jones RH, O'Donnell C, Brown JL, Green S, Sullivan
43 H, Hedlund T, Crawford ED. The metabolites citrate, myo-inositol, and spermine are
44 potential age-independent markers of prostate cancer in human expressed prostatic
45 secretions. *Prostate* 2008 May 1;68(6):620-8.
46
47 37. Griffin JL, Shockcor JP. Metabolic profiles of cancer cells. *Nat Rev Cancer*
48 2004;4:551–561.
49
50
51
52
53
54
55
56
57
58
59
60

1
2
3 38. Koochekpour S. Glutamate, a metabolic biomarker of aggressiveness and potential
4 therapeutic target for prostate cancer. Asian J Androl 2013 Mar;15(2):212-3.
5
6

7 39. Lange T, Schulte RF, Boesiger P. Quantitative J-resolved prostate spectroscopy using
8 two-dimensional prior-knowledge fitting. Magn Reson Med 2008 May;59(5):966-72.
9
10
11
12
13
14
15
16
17
18
19
20
21
22
23
24
25
26
27
28
29
30
31
32
33
34
35
36
37
38
39
40
41
42
43
44
45
46
47
48
49
50
51
52
53
54
55
56
57
58
59
60

Table 1. Measures of Sensitivity, Specificity, PPV, NPV, and Accuracy of MaxEnt and TV Method using ROC Curve Analysis

MaxEnt						
Metabolites	Sensitivity %	Specificity %	Accuracy %	PPV %	NPV %	AUC %
Cit	86.4	86.4	86.4	86.4	86.4	94.0
Glx	40.9	59.1	50.0	50.0	50.0	48.0
mI	63.6	63.6	63.6	63.6	63.6	65.0
Spm	81.8	40.9	61.4	56.7	64.3	64.9
TV						
Cit	86.4	86.4	86.4	86.4	86.4	92.1
Glx	54.5	47.6	51.2	52.2	50.0	50.6
mI	50.0	38.1	44.2	45.8	42.1	50.6
Spm	77.3	40.9	59.1	58.1	69.2	58.5

Figure Legends

1. Fig.1. Schematic diagram of 4D EP-JRESI pulse sequence.
2. Fig.2. Metabolite ratios of Cit, Spm, mI and Glx in cancer and non-cancer locations processed by MaxEnt.
3. Fig.3. Metabolite ratios of Cit, Spm, mI and Glx in cancer and non-cancer locations processed by TV.
4. Fig.4. Spatial map of (Ch +Cr) for TV and MaxEnt reconstructions of 4D EP-JRESI data recorded in a 74 year old PCa patient.
5. Fig.5. 2D JPRESS spectra extracted from an EP-JRESI voxel (A) after the MaxEnt and TV reconstructions of cancer (B&D) and non-cancer (C&E) locations.
6. Fig.6. Correlation of MaxEnt and TV for Cit, Glx, mI and Spm in cancer locations.

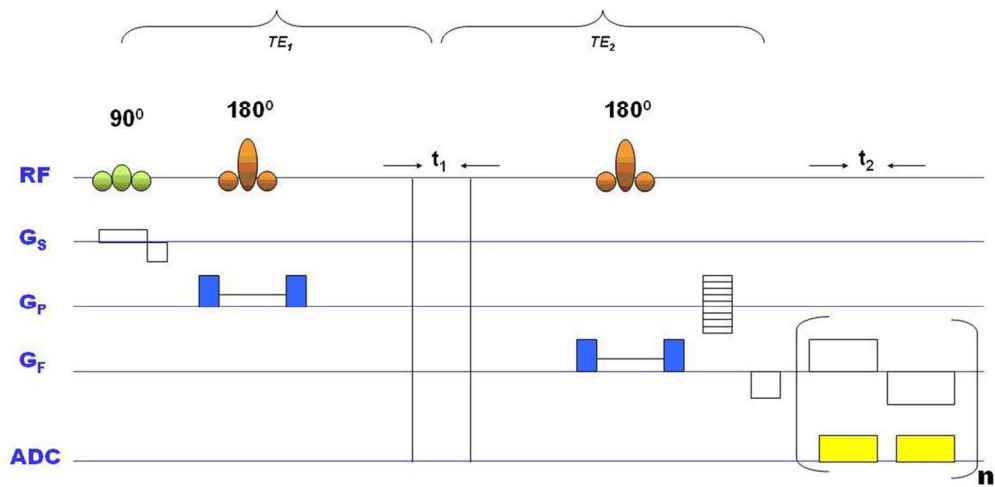


Fig.1. Schematic diagram of 4D EP-JRESI pulse sequence.
116x58mm (300 x 300 DPI)

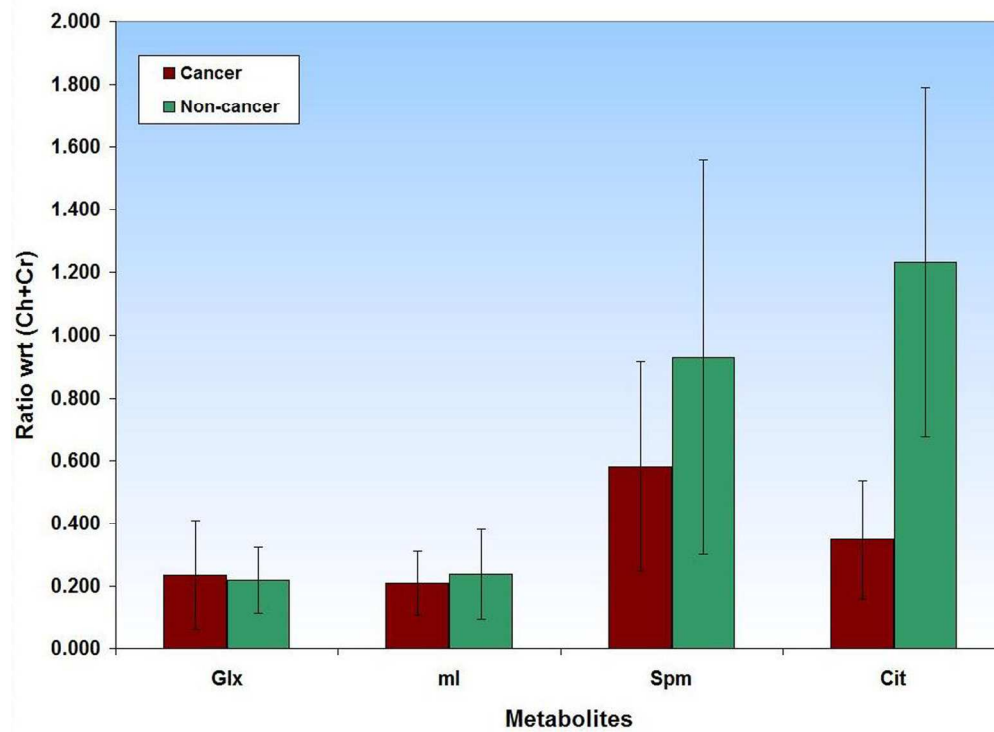


Fig.2. Metabolite ratios of Cit, Spm, mI and Glx in cancer and non-cancer locations processed by MaxEnt.
156x114mm (300 x 300 DPI)

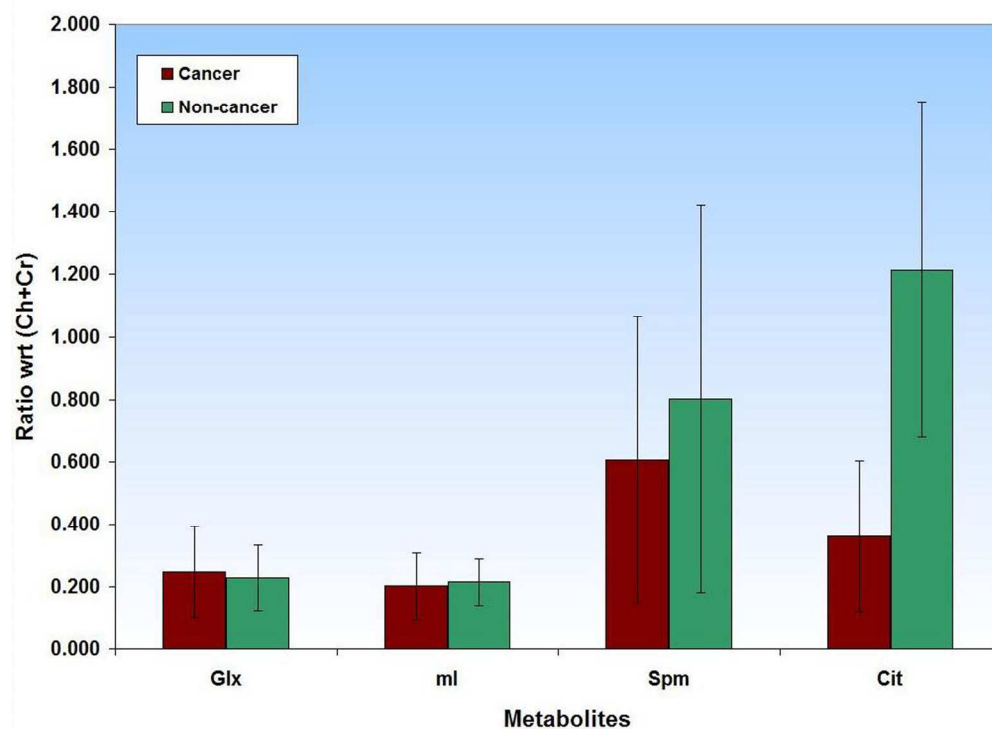


Fig.3. Metabolite ratios of Cit, Spm, mI and Glx in cancer and non-cancer locations processed by TV.
157x115mm (300 x 300 DPI)

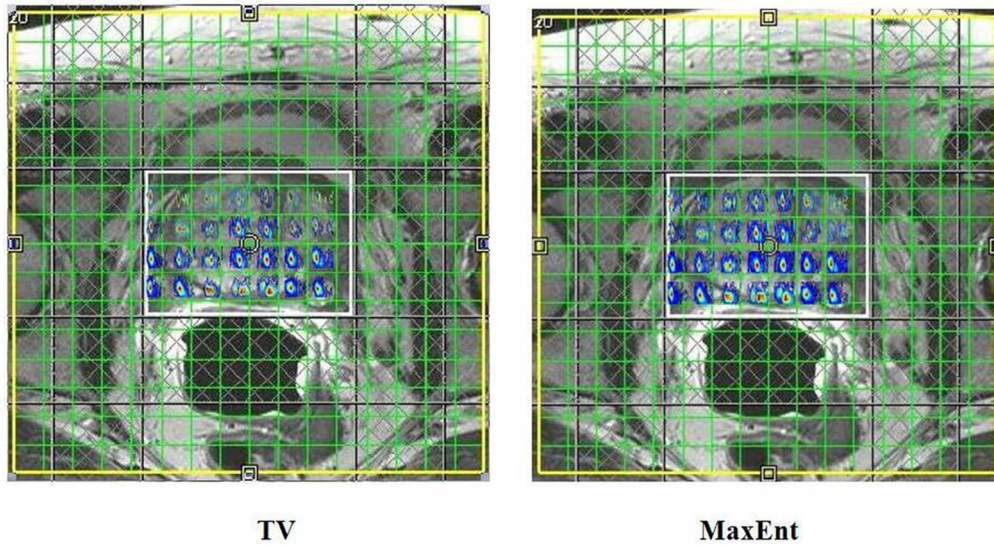


Fig.4. Spatial map of (Ch +Cr) for TV and MaxEnt reconstructions of 4D EP-JRESI data recorded in a 74 year old PCa patient.
104x56mm (300 x 300 DPI)

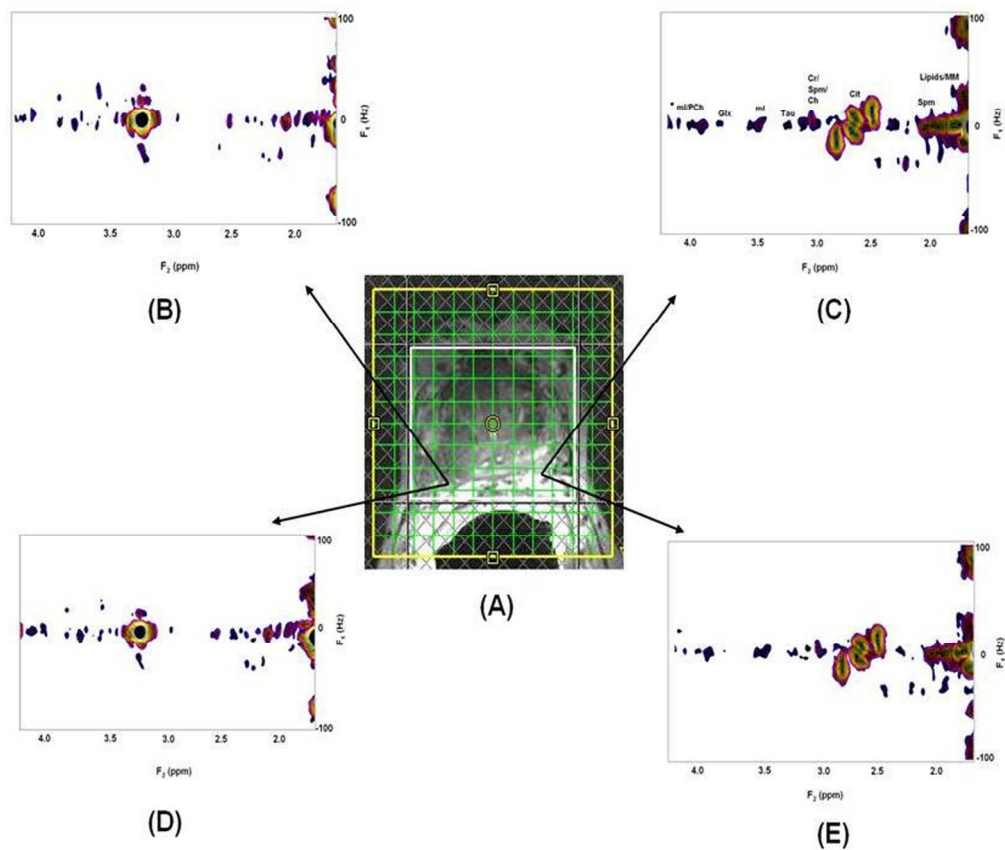


Fig.5. 2D JPRESS spectra extracted from an EP-JRESI voxel (A) after the MaxEnt and TV reconstructions of cancer (B&D) and non-cancer (C&E) locations.
148x126mm (300 x 300 DPI)

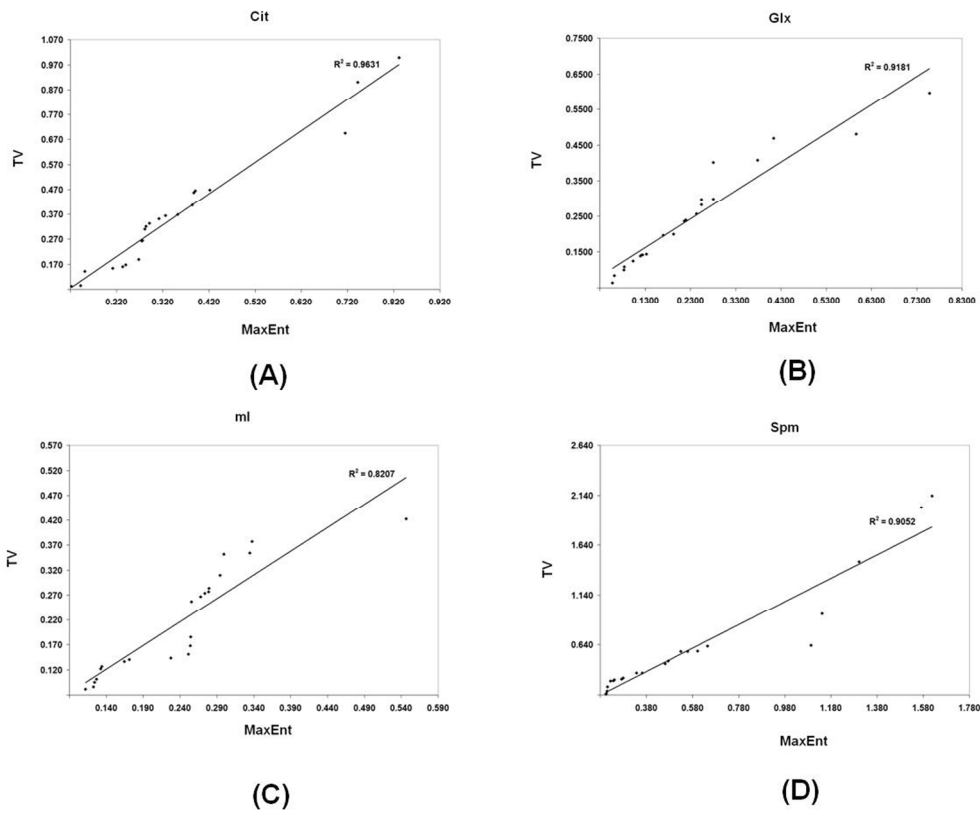


Fig.6. Correlation of MaxEnt and TV for Cit, Glx, mI and Spm in cancer locations. 197x161mm (300 x 300 DPI)